

This article was downloaded by:

On: 26 January 2011

Access details: *Access Details: Free Access*

Publisher *Taylor & Francis*

Informa Ltd Registered in England and Wales Registered Number: 1072954 Registered office: Mortimer House, 37-41 Mortimer Street, London W1T 3JH, UK



## Liquid Crystals

Publication details, including instructions for authors and subscription information:

<http://www.informaworld.com/smpp/title~content=t713926090>

### Freedericksz transition of planar oriented smectic C phases

G. Pelzl<sup>a</sup>; P. Schiller<sup>a</sup>; D. Demus<sup>a</sup>

<sup>a</sup> Sektion Chemie der Martin-Luther-Universität Halle-Wittenberg, WB Physikalische Chemie, DDR-402S Halle/S., Mühlpforte 1, G.D.R.

**To cite this Article** Pelzl, G. , Schiller, P. and Demus, D.(1987) 'Freedericksz transition of planar oriented smectic C phases', *Liquid Crystals*, 2: 2, 131 – 148

**To link to this Article:** DOI: 10.1080/02678298708086286

**URL:** <http://dx.doi.org/10.1080/02678298708086286>

PLEASE SCROLL DOWN FOR ARTICLE

Full terms and conditions of use: <http://www.informaworld.com/terms-and-conditions-of-access.pdf>

This article may be used for research, teaching and private study purposes. Any substantial or systematic reproduction, re-distribution, re-selling, loan or sub-licensing, systematic supply or distribution in any form to anyone is expressly forbidden.

The publisher does not give any warranty express or implied or make any representation that the contents will be complete or accurate or up to date. The accuracy of any instructions, formulae and drug doses should be independently verified with primary sources. The publisher shall not be liable for any loss, actions, claims, proceedings, demand or costs or damages whatsoever or howsoever caused arising directly or indirectly in connection with or arising out of the use of this material.

## Freedericksz transition of planar oriented smectic C phases

by G. PELZL, P. SCHILLER and D. DEMUS

Sektion Chemie der Martin-Luther-Universität Halle-Wittenberg,  
WB Physikalische Chemie, DDR-4020 Halle/S., Mühlpforte 1, G.D.R.

(Received 6 October 1986; accepted 27 November 1986)

The Freedericksz transition of planar oriented smectic C phases has been investigated experimentally. The optical picture of the effect observed under a polarizing microscope is described in detail. For a number of selected materials the threshold voltage and the switching times were measured. The experimental data were used to estimate the elastic constant and the rotational viscosity of smectic C phases. The experimental results are discussed and interpreted theoretically.

### 1. Introduction

The possibility of field-induced reorientations in smectic C phases was first considered by Rapini [1] for a number of important geometrical cases. Depending on the boundary conditions of the substrates and the direction of the field, Rapini predicted two kinds of field-induced transitions. The first kind is characterized by a distortion of the smectic layers. Because of the quasi-incompressibility of the smectic layers the amplitudes of the deformations should be very small and should increase only slightly with increasing field strength, so that it is probably impossible to detect this transition experimentally. For this reason Rapini called this effect a 'ghost' transition.

In addition, another type of field-induced reorientation is possible based on the rotation of the director around the layer normal. Rapini studied the threshold behaviour in the framework of the continuum theory for selected geometrical cases. However in these investigations only continuous transitions were taken into account which are characterized by a continuous increase of the deformation above a critical threshold field. In 1977 Meirovich *et al.* [2] were able to show by theoretical investigations that in smectic C phases discontinuous transitions can also occur. In these cases at the threshold the director is reoriented discontinuously by a finite amount from its initial position.

In 1979 we were first able to observe a dielectric reorientation of a planar-oriented smectic C phase exhibiting positive dielectric anisotropy [3, 4]. In the planar-oriented sample the director is aligned uniformly parallel to the substrate planes. On applying an electric field perpendicular to the director a deformation of the sample was detected which is caused by the rotation of the director within the smectic layers around the layer normal. In analogy to the corresponding reorientation of planar oriented nematic phases we called this transition a Freedericksz transition [5].

In the first part of this paper the Freedericksz transition of planar-oriented smectic C phases is discussed from a theoretical point of view. For different kinds of planar alignment distinguished by the orientation of the layer normal the threshold behaviour is treated theoretically. In addition, the dynamic behaviour of the switching process is discussed.

In §3 the experimental devices and the manufacture of planar-oriented samples are briefly described. Section 4 presents a summary of the most important results of the experimental investigations. It is shown that the optical picture of the Fredericksz transition in the smectic C observed under a polarizing microscope is quite similar to that in nematic phases. The rotation of the director around the layer normal is detected by a simple optical method. For a number of materials the threshold voltage as well as the switching times of the Fredericksz transition are used to determine the elastic constant and the rotational viscosity in smectic C phases. The experimental results are discussed and interpreted theoretically.

## 2. Theoretical considerations

### 2.1. Structure

In smectic C phases the molecules are arranged in a layered structure. The preferred direction of the long molecular axes (that is the director  $\mathbf{U}$ ) is tilted with respect to the layer normal by an angle  $\theta$  (cf. figure 1). On applying an electric or a magnetic field the director  $\mathbf{U}$  can rotate around the layer normal without distortion of the smectic planes. On rotation  $\mathbf{U}$  is confined to the surface of a cone with aperture  $2\theta$ . The projection of  $\mathbf{U}$  on to the smectic layer plane and a fixed vector  $\boldsymbol{\xi}$  define an azimuthal angle  $\Phi$  varying between  $-\pi$  and  $+\pi$ .

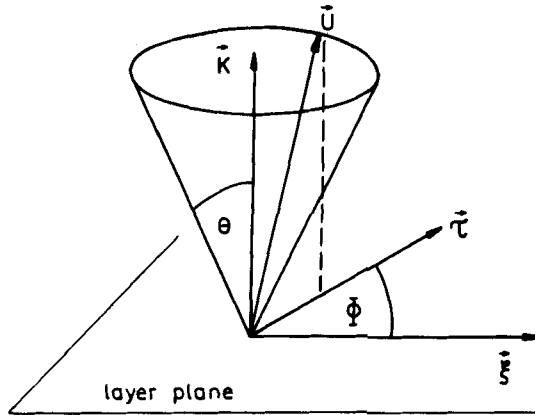


Figure 1. Orientation of the director with respect to the smectic layer plane.  $\mathbf{U}$ , director;  $\mathbf{K}$ , layer normal;  $\theta$ , tilt of the director;  $\boldsymbol{\tau}$ , unit vector oriented parallel to the projection of  $\mathbf{U}$  on the smectic layer plane;  $\boldsymbol{\xi}$ , fixed vector lying on the smectic layer plane;  $\Phi$ , rotation angle of  $\boldsymbol{\tau}$ .

Figure 2 shows the alignment of the director in the sample surface. The surface of the lower substrate is chosen to be identical to the  $yz$  plane of a cartesian system of coordinates. The normal  $\mathbf{K}$  of the smectic layer planes and the fixed vector  $\boldsymbol{\xi}$  lie within the  $xy$  plane which is perpendicular to the boundaries. The lower plane and  $\mathbf{K}$  enclose the angle  $\mu$ . We obtain by simple geometrical considerations

$$\cos \Phi_0 = \frac{\tan \mu}{\tan \theta}, \quad (1)$$

which determines the azimuthal angle  $\Phi$  at the plates ( $x = 0$  and  $x = D$ ) for planar boundary conditions. The borderline cases characterized by  $\mu = \theta$  and  $\mu = 0$  are shown in figure 3.

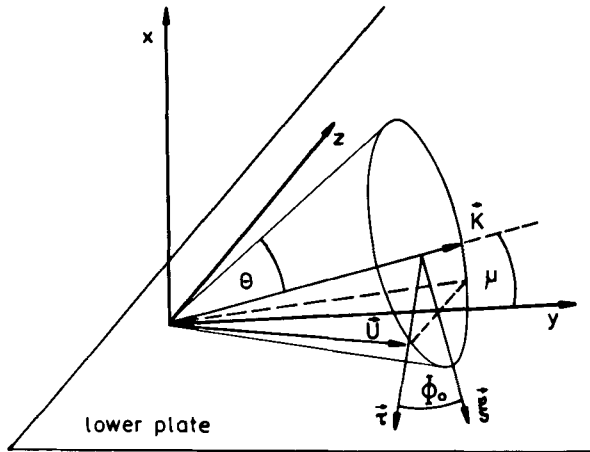
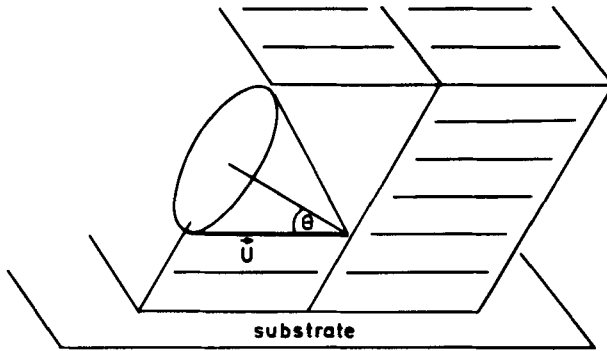
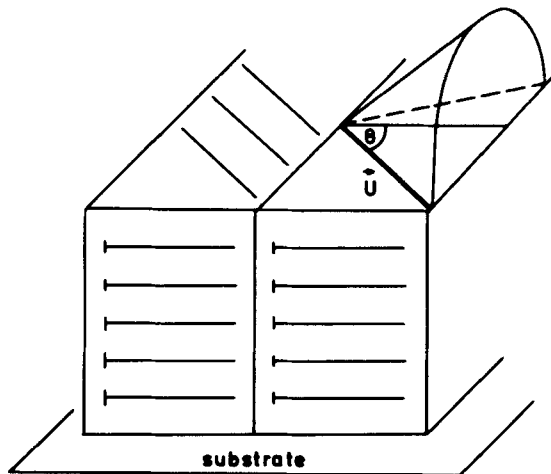


Figure 2. Planar alignment of the director at the substrate.  $x$ ,  $y$  and  $z$  define a cartesian system of coordinates.  $\mu$ , tilt angle of the layer normal with respect to the substrate;  $\Phi_0$ , angle between  $\tau$  and  $\zeta$  on the substrate surface  $x = 0$ ;  $\mathbf{U}$ ,  $\mathbf{K}$ ,  $\tau$  and  $\zeta$  are defined as in figure 1.



(a)



(b)

Figure 3. Borderline cases of planar alignment (a) the director and the layer normal are in a plane perpendicular to the substrate plane; (b) the director and the layer normal are in the substrate plane.

## 2.2. Free energy

If distortions of the smectic layer planes are neglected, the free curvature elastic energy due to director rotations includes four elastic constants. In a simplified model only two elastic constants  $B_{\parallel}$  and  $B_{\perp}$  are introduced by referring to distortions with gradients parallel ( $\nabla_{\parallel}\Phi$ ) and perpendicular ( $\nabla_{\perp}\Phi$ ) to the smectic layers, respectively. Then the elastic energy density is obtained as

$$f_1 = \frac{1}{2}B_{\parallel}(\nabla_{\parallel}\Phi)^2 + \frac{1}{2}B_{\perp}(\nabla_{\perp}\Phi)^2. \quad (2)$$

In our special geometry (cf. figure 2) we obtain, for distortions with gradients parallel to the  $x$  axis,

$$f_1 = \frac{1}{2}B \left( \frac{\partial\Phi}{\partial x} \right)^2, \quad (3)$$

with

$$B = B_{\parallel} \cos^2 \mu + B_{\perp} \sin^2 \mu.$$

To a good approximation the dielectric susceptibility tensor is axially symmetric with its unique axis parallel to  $\mathbf{U}$ . As for nematics the anisotropic part of the electric field energy is

$$f_2 = -\frac{\Delta\varepsilon \varepsilon_0}{2} (\mathbf{U} \cdot \mathbf{E})^2. \quad (4)$$

Here we assume that the dielectric anisotropy  $\Delta\varepsilon$  is positive. Note that the electric field  $E$  is not strongly dependent on  $x$  since the effective value  $\Delta\varepsilon \sin^2 \theta$  of the dielectric anisotropy is usually small compared to the dielectric susceptibility,  $\varepsilon_{\perp}$ , perpendicular to the director. Using angles defined in figure 2  $f_2$  is given explicitly as

$$f_2 = -\frac{\Delta\varepsilon \varepsilon_0 E^2}{2} \sin^2 \theta \cos^2 \mu (\cos \Phi - \cos \Phi_0)^2. \quad (5)$$

The overall free energy of a sandwich cell with thickness  $D$

$$F = A \int_0^D dx (f_1 + f_2) \quad (6)$$

(where  $A$  is the area of the slab) is a minimum for an equilibrium configuration. From this condition the eulerian equation

$$B \frac{\partial^2 \Phi}{\partial x^2} = \Delta\varepsilon \varepsilon_0 E^2 \sin^2 \theta \cos^2 \mu (\cos \Phi - \cos \Phi_0) \sin \Phi \quad (7)$$

is derived.

It is convenient to introduce an angle  $\Phi^*$  defined by

$$\Phi^* = -\Phi_0 + \Phi, \quad (8)$$

which is zero at the boundaries of the cell (corresponding to strong surface anchoring).

Using  $\Phi^*$  the free energy in equations (6) and (7) take the form

$$F = \frac{1}{2}AB \int_0^D dx \left\{ \left( \frac{\partial\Phi^*}{\partial x} \right)^2 - \frac{h^2}{D^2} [\cos(\Phi^* + \Phi_0) - \cos \Phi_0]^2 \right\} \quad (9)$$

and

$$\frac{\partial^2 \Phi^*}{\partial x^2} = \frac{h^2}{D^2} [\cos(\Phi^* + \Phi_0) - \cos \Phi_0] \sin(\Phi^* + \Phi_0), \quad (10)$$

with the dimensionless parameter

$$h = \sqrt{\left(\frac{\epsilon_0 \Delta \epsilon}{B}\right)} \sin \theta \cos \mu D E. \quad (11)$$

### 2.3. Threshold field of the Fredericksz transition

We first discuss the borderline case with  $\mu = 0$  ( $\Phi_0 = \pi/2$ ). Here the mathematical equivalence of equation (10) to the corresponding equation for a Fredericksz transition of a nematic layer [6] is obvious. Accordingly, the smectic C slab exhibits a Fredericksz transition like its nematic counterpart at the threshold  $h_C = \pi$  or

$$E_C = \frac{\pi}{\sin \theta D} \sqrt{\left(\frac{B}{\Delta \epsilon \epsilon_0}\right)}. \quad (12)$$

The transition above  $E_C$  is continuous, i.e. deformations in the cell grow gradually with increasing field (cf. figure 4).

In all other cases, if  $\mu \neq 0$  the Fredericksz transition is discontinuous and the solution of equation (10) is more complicated. To characterize discontinuous transitions three different field strengths can be defined [2]. At small fields,  $E$ , below  $E_1$  only the homogeneous undistorted configuration of the sample is possible. In contrast, at sufficiently large fields above a definite value  $E_3$ , a strongly distorted director configuration represents the only stable state. Within an intermediate region  $E_1 < E < E_3$  the system is bistable (cf. figure 4), because both the homogeneous and the distorted state correspond to minima of the free energy. There is a definite field  $E_2$  in this region which satisfies the equilibrium condition

$$F'(E_2) = F''(E_2), \quad (13)$$

where  $F'$  and  $F''$  are the free energies of the homogeneous and the distorted state, respectively.

Director reorientations in smectic C slabs subjected to a magnetic field were first investigated theoretically by Meirovich *et al.* [2]. Although they referred to slabs with

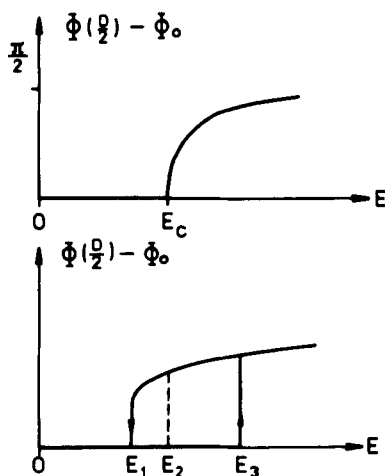


Figure 4. The rotation angle  $\Phi(D/2)$  in the middle plane at  $x = D/2$  of the sandwich cell is plotted schematically against the electric field strength  $E$ . For continuous Fredericksz transitions (upper diagram) a unique threshold  $E_C$  exists. For a discontinuous transition the system is bistable within a region between  $E_1$  and  $E_3$  (lower diagram).

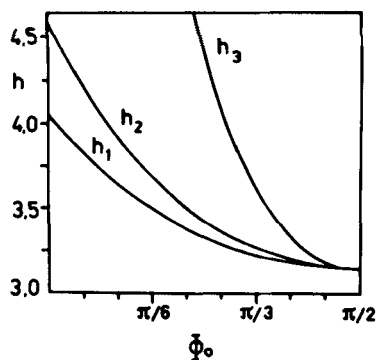


Figure 5. Threshold of the Fredericksz transition in dependence of  $\Phi_0$  (after figure 6 in [2]).  
 $h = (\epsilon_0 \Delta \epsilon / B)^{1/2} \sin \theta \cos \mu D E$ ;  $\Phi_0 = \arccos(\tan \mu / \tan \theta)$ .

smectic layers parallel to the substrate surface the essential results remain valid for planar cells. In both cases the free energies of the cell are equivalent from a mathematical point of view, when the field is perpendicular to the initial director orientation. This condition is always satisfied in our planar geometry. Accordingly the results of numerical computations published in [2] can be applied to the present case. Figure 5 shows a plot of the parameters  $h_1$ ,  $h_2$  and  $h_3$  against  $\Phi_0$  which are related to  $E_1$ ,  $E_2$  and  $E_3$ , respectively (cf. equation (11)). According to equation (1) the borderline case  $\mu = 0$  corresponds to  $\Phi_0 = \pi/2$  and  $\mu = \theta$  to  $\Phi_0 = 0$ . Only for a continuous Fredericksz transition do the three field strengths coincide ( $E_1 = E_2 = E_3$  if  $\mu = 0$ ). Increasing  $E$  slowly, at  $\mu \neq 0$  the onset of the director reorientation can occur at a field between  $E_2$  and  $E_3$  (metastable region of the homogeneous state). Mostly, in our experiments, the second borderline case  $\mu = \theta$  was established approximately. If  $\mu$  approaches  $\theta$  the field  $E_3$  tends to infinity, on the other hand  $E_2$  is finite (cf. figure 5). As thermal fluctuations are not sufficient to overcome the relatively high energy barrier between the homogeneous and the distorted state, pronounced hysteresis effects should be observable in the bistable region  $E_1 < E < E_3$ . On varying the applied field slowly distortions may appear and vanish at thresholds, which are different from each other. Surprisingly, we found experimentally bistability only in a few cases [7]. In our view small deviations from the planar alignment at the plates enable the director to switch to its absolutely stable configuration characterized by the global minimum of the free energy. According to the terminology of catastrophe theory [8], the Maxwell convention is satisfied in our case. In this case the unique threshold of the Fredericksz transition is the field  $E_2$  which is given for the borderline case  $\mu = \theta$  by the formula [9]

$$E_2 = \frac{4.5}{D \sin \theta \cos \theta} \sqrt{\left(\frac{B}{\epsilon_0 \Delta \epsilon}\right)}. \quad (14)$$

The threshold for  $\mu = \theta$  computed by Meirovich *et al.* [2] is a few per cent higher (cf. figure 5). But this small difference is not relevant from a physical point of view.

#### 2.4. Dynamic behaviour

Switching processes may be described by adding a viscous torque to equation (10). For  $E = 0$  we obtain

$$B \frac{\partial^2 \Phi^*}{\partial x^2} - \lambda \frac{\partial \Phi^*}{\partial t} = 0, \quad (15)$$

where  $\lambda$  is the rotational viscosity. According to equation (15), at zero field an initial deformation  $\Phi^* \sim \sin(\pi x/D)$  decays exponentially with the time constant

$$t_{\text{decay}} = \frac{\lambda D^2}{B\pi^2} \quad (16)$$

in complete analogy to a nematic layer [6].

A simple formula describing the device response to an external field is only found for the borderline case with  $\mu = 0$ . Here an initial disturbance  $\Phi^* \sim \sin(\pi x/D)$  grows exponentially with the time constant

$$t_{\text{rise}} = \frac{\lambda}{\Delta\varepsilon \sin^2\theta (E^2 - E_C^2)} \quad (17)$$

immediately after applying an electric field  $E > E_C$ .

### 3. Experimental

#### 3.1. Measuring devices

For the electro-optical studies the liquid-crystalline materials were sandwiched between two glass plates which were coated with a transparent conductive layer on the inner side. The distance between the plates (mostly  $10\ \mu\text{m}$ ) was fixed by mylar spacers. The sample was placed on the heating stage of a polarizing microscope (Ergaval, VEB Carl Zeiss, Jena). To induce dielectric reorientation the cell was subjected to an a.c. field. The voltage of the desired frequency (mostly 1–2 kHz) was generated by a RC generator (GF 20, Clamann and Grahnert, Dresden) or by a function generator (TR-0452, Hungary).

The threshold voltage of the Fredericksz transition in the nematic and smectic phase was determined from the experimental light intensity-voltage curve. The light intensity dependence on the voltage was measured by a photomultiplier (M 10 FS 29, VEB Werk für Fernsehelektronik, Berlin) which was placed on the microscope tube.

The measurement of the switching times was performed with a device which is shown schematically in figure 6. The field induced change of the light intensity was

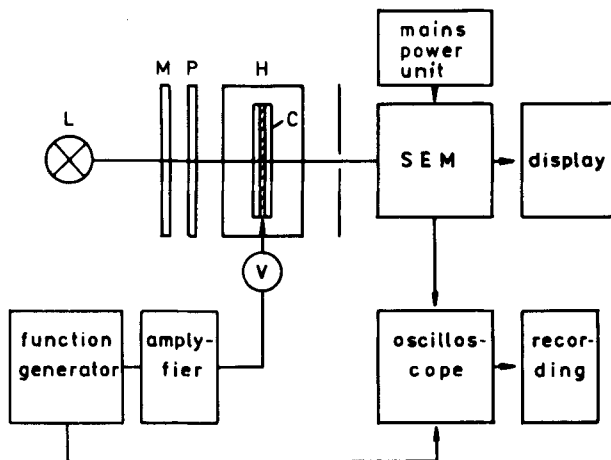


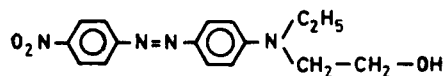
Figure 6. The experimental equipment. L, light source; M, monochromator; P, polarizer; C, cell; H, heating device; SEM photomultiplier.



monitored by the photomultiplier the output of which was linked to a storage oscilloscope (C8-13, U.S.S.R.). The voltage was generated by the function generator as a rectangular impulse. By means of an amplifier voltages up to 60 V were generated. The function generator was connected directly with the trigger entrance of the oscilloscope. In this way the simultaneous voltage change in the cell and the start of the oscilloscope sweep was guaranteed.

### 3.2. Planar oriented samples of smectic C phases

As described elsewhere [4, 10] planar oriented smectic C phases can be obtained by very slow cooling of the planar oriented nematic phase into the smectic state. By microscopic observation the textures of the smectic A and of the smectic C phase show only some poorly contrasted traces of focal conics with very elongated ellipses. The homogeneity of the planar orientation could be proved by the investigation of the dichroism for a dissolved dichroic dye (WO 4)



The electronic transition of the dye molecule responsible for the absorption band at 505 nm is directed parallel to the molecular long axis (*p* dye). As the dissolved dye molecules are oriented parallel to the director, the electric vector of the linearly polarized light, for which the maximum absorption is found in the wavelength region of the dye absorption, coincides with the projection of the director in the substrate plane. We found that this alignment is unchanged at the transition of the nematic phase into the smectic A or C phases. Furthermore, the dichroic ratio, the ratio of the optical densities parallel and perpendicular to the director, increases at the transition from the nematic into the smectic phases. We conclude from these results that not only the projection of the director on to the substrate plane but also the direction of the director itself is the same in the nematic phase and in the smectic A or C phases.

It should be emphasized that the term *planar* is not sufficient to designate the orientation of a smectic C phase because samples with the same alignment of the director can be distinguished by a different orientation of the layer normal. As demonstrated in figure 2 the orientation of the layer normal **K** can be described by the angle  $\mu$  which is enclosed between **K** and the substrate plane. The two borderline cases of the planar alignment characterized by  $\mu = \theta$  and  $\mu = 0$ , respectively, are shown in figures 3(a) and (b). The intermediate general case corresponds to  $0 < \mu < \theta$ . In our studies it was found (see §4.1) that in most cases this intermediate case was realized, but the orientation was not too different from the first borderline case ( $\mu = \theta$ ). The second borderline case could be clearly detected for one material only.

## 4. Experimental results

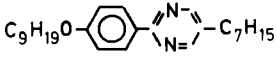
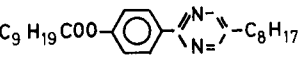
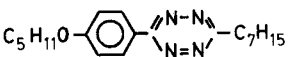
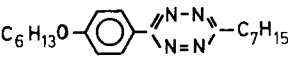
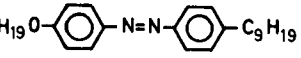
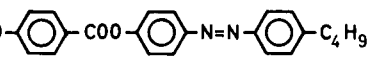
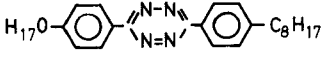
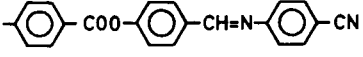
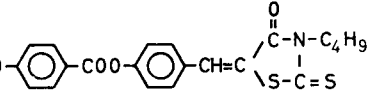
### 4.1. Optical observations

The Freedericksz transition of a planar oriented smectic C phase was observed under a polarizing microscope. As first described in [4] above the threshold voltage homogeneously deformed regions with a uniform interference colour appear indicating the uniform, average orientation of **U** and **K**. With increasing voltage the interference colour is changed within the single regions or domains, not only because of a change of the optical path difference but also because of the change of the azimuthal angle between the polarizers and the optic axes. In most cases two kinds of deformed

regions are observed which show a different interference colour and are separated by inversion walls. This situation is illustrated in figure 7 for the planar oriented smectic C phase of 5-*n*-heptyl-2-[4-*n*-nonyloxyphenyl]-pyrimidine (compound C1 in table 1). For comparison, in figure 8 we present the Fredericksz transition of a non-oriented smectic C phase, where a broken fan-shaped texture is observed.

In some cases nearly the entire sample was reoriented as a uniform region. Generally it should be noted that the optical picture of the Fredericksz transition in smectic C phases is quite similar to that of nematic phases.

Table 1. The characteristics of the liquid crystals studied.

Compound	transition temperatures (in °C)	References	Phase	$T/^\circ\text{C}$	$U_2/V$
C1			N $S_C$	62 49	6 17
K	45.5 $S_C$ 51 $S_A$ 56.5 N 69.5 I	[13]	$S_C$	31	17.5
C2			N $S_C$	57 53.5	5 17
K	42 $S_C$ 55.5 N 59.8 I	[14]	$S_C$	37	17
C3			N $S_C$	53 51	6 10
K	49 $S_C$ 52.5 N 63 I	[15]	$S_C$	44	13
C4			N $S_C$	75 66	5 21
K	58 $S_C$ 67 $S_A$ 74 N 76 I	[15]	$S_C$	54	24.5
C5			N $S_C$	81.5 71.5	6 33
K	51 $S_1$ 51.5 $S_C$ 72.5 $S_A$ 80.8 N 83 I	[16, 17]	$S_C$	53.5	37
C6			N $S_C$	100 94	10 14
K	84.5 $S_C$ 95.3 N 193.5 I	[18]	$S_C$	74	18
C7			N $S_C$	164 159	8 16
K	127 $S_C$ 162.5 N 172.5 I	[3]	$S_C$	134.5	18
C8			N $S_C$	234 75	2 4
K	100 ( $N_{re}$ 66 $S_C$ 79) $S_A$ 232 N 242 I	[19]			
C9			N $S_C$	116 70	4 15
K	104.5 ( $S_C$ 72.5) $S_A$ 114.5 N 120 I	[20]	$S_C$	62.5	20

K, solid crystal; N, nematic;  $N_{re}$ , re-entrant nematic;  $S_A$ ,  $S_C$ ,  $S_1$ , smectic A, C, I; I, isotropic liquid.

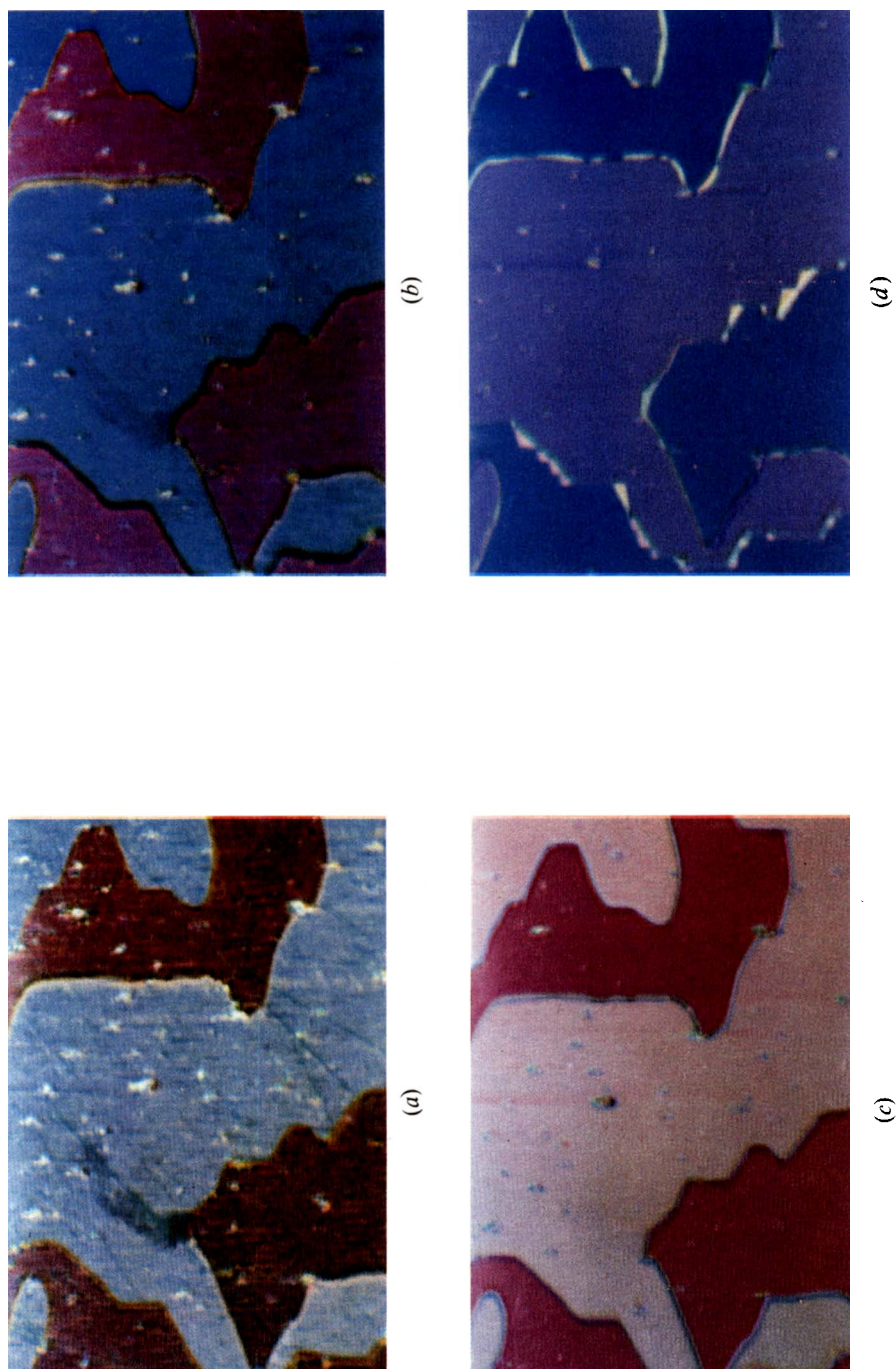


Figure 7. Fredericksz transition of the planar oriented smectic C phase of 5-*n*-heptyl-2-[4-*n*-nonyloxyphenyl]-pyrimidine (C1) observed between crossed polarizers at different voltages (a) 18 V, (b) 20 V, (c) 25 V, (d) 50 V (threshold voltage 17 V;  $T$ , 38°C;  $D$ , 10  $\mu\text{m}$ ; magnification 88  $\times$ ).

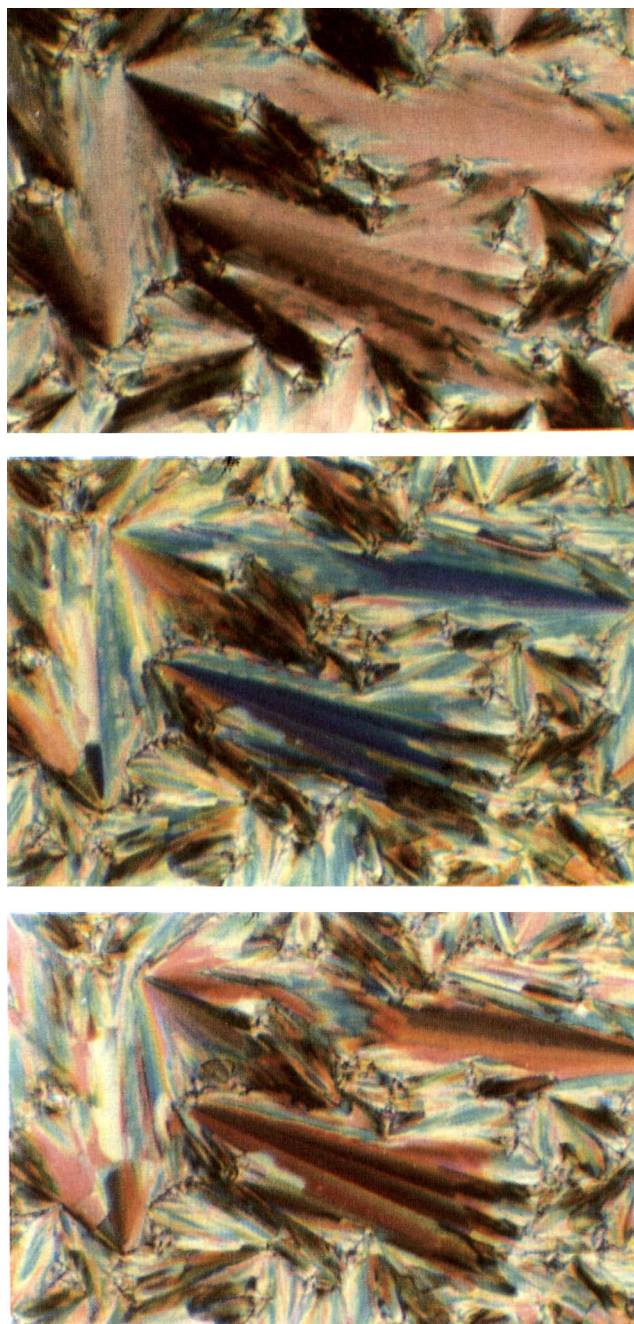


Figure 8. Dielectric reorientation of the smectic C broken fan-shaped texture of 5-*n*-nonyl-2-[4-*n*-octyloxyphenyl]-pyrimidine (K 33  $S_C$  60  $S_A$  74.5 I) (a) off state, (b) on state (50 V), (c) on state (75 V) (threshold voltage 17 V;  $T$ , 38°C;  $D$ , 10  $\mu\text{m}$ ; magnification 160 $\times$ ).

To detect the field induced rotation of the director 0.5 wt % of the *p* dye WO4 was dissolved in the liquid crystal. The average orientation of the director projection on to the substrate plane can be determined from the vibration direction of linearly polarized light for which maximum absorption is observed in the wavelength region of dye absorption. For a given deformed region we found that above the threshold voltage with increasing voltage the projection of the director on to the substrate plane is changed with respect to its original projection up to a maximum angle  $\beta_1$ . With further increasing voltage this angle again decreases to zero (figure 9(a)). In many cases at high voltages the projection of the director is shifted in the reverse direction up to a maximum angle  $\beta_1$  (see figure 9(c)). In neighbouring deformed domains the angles  $\beta_1$  and  $\beta_2$  are nearly the same but the change of the director projection takes place in an inverse direction. Only for one substance namely 4-*n*-nonyloxy-benzoyloxy-4'-*n*-azobenzene (compound C6 in table 1) did we observe a completely different behaviour. In this case the projection of the director on to the substrate plane is shifted in one direction only up to a maximum angle  $\beta$  and remains in this position also at high voltages (see figure 9(b)).

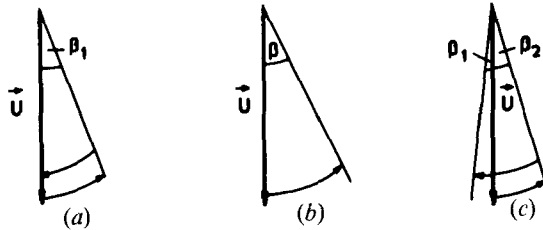


Figure 9. Change of the projection of the director  $\mathbf{U}$  on to the substrate plane with respect to its original position.

Generally, the change of the director projection with increasing voltage is accompanied by a decrease of the light absorption caused by the greater alignment of the dye molecules in the field direction.

A typical change of the projection of  $\mathbf{U}$  on to the substrate plane can be interpreted by a simple model which is shown in figure 2. The director,  $\mathbf{U}$ , is aligned parallel to the bounding substrate which corresponds to the  $yz$  plane of the cartesian coordinate system. The  $x$  direction coincides with the direction of the electric field. The possible orientations of the layer normal  $\mathbf{K}$  are described by the angle  $\mu$ , which is enclosed between  $\mathbf{K}$  and the substrate plane. On applying an electric field perpendicular to the director, above the threshold field the director tends to align as far as possible in the field direction because of the positive dielectric anisotropy of the sample. Provided that the smectic layers are neither distorted nor shifted by the electric field the director rotates around the layer normal on the surface of the cone shown in figure 2.

The field-induced rotation of  $\mathbf{U}$  on the cone changes the projection of  $\mathbf{U}$  on to the substrate plane with respect to the original direction. Depending on the starting orientation of the layer normal  $\mathbf{K}$  characterized by the angle  $\mu$ , the projection of  $\mathbf{U}$  is changed in a different manner. As seen from figure 2 the first borderline case of planar orientation ( $\mu = \theta$ ) leads to a situation shown in figure 9(a), whereas  $\mu = 0$  and  $0 < \mu < \theta$  correspond to the cases shown in figures 9(b) and (c), respectively. It should be noted that from the experimentally available angles  $\beta_1$  and  $\beta_2$  shown in figure 9 the tilt angle of the smectic C phase can be determined [4].

#### 4.2. Measurement of the threshold voltage

For a number of materials the threshold voltage of the Fredericksz transition in smectic C phases was determined from the experimental light intensity-voltage curves. The results are presented in table 1. For comparison, the threshold voltage of the Fredericksz transition in the nematic phase is given for a temperature near to the smectic A–nematic or smectic C–nematic transition, respectively. It is seen from the table that the threshold voltage in the smectic C phase is about 1.5 to 5 times larger than in the nematic phase of the same substance. The low threshold voltage of 4-*n*-decyloxy-benzoyloxy-benzyliden-4'-cyanoaniline (C8) is remarkable.

As described in the previous section only for the 4-*n*-nonyloxy-benzoyloxy-4'-*n*-butylazobenzene (C6) was the second borderline case of planar alignment ( $\mu = 0$ ) clearly detected. In this case the Fredericksz transition takes place as a continuous transition and the threshold field is given by equation (10). For the other substances listed in table 1 the planar alignment corresponds to the first borderline case ( $\mu = \theta$ ) or is not too different from this. As discussed in §2.3 a discontinuous transition is predicted by the theory for such orientations. According to the theory the director reorientation should occur in the bistable region between the stability limits  $E_1$  and  $E_3$  of the distorted and homogeneous state, respectively (cf. figure 4). Only in a few cases could we establish bistability experimentally; these results are to be published elsewhere). In general the same threshold for the director reorientation is observed when the field is increased slowly or decreased. From this observation we conclude that the Maxwell convention is satisfied and in our samples the threshold field of the discontinuous Fredericksz transition is determined by the equality of the free energies for the homogeneous and the distorted configuration. For the first borderline case ( $\mu = \theta$ ) this threshold  $E_2$  is given by equation (14). For  $0 < \mu < \theta$  the threshold field  $E_2$  can be obtained from figure 5. In accordance with equations (12) and (14) we found that the threshold field is independent of the layer thickness. As reported earlier [10, 11] the frequency dependence of the threshold voltage in a smectic C is quite similar to that in the nematic phase and can be expressed by an analogous formula, as derived for nematics.

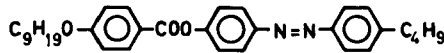
The threshold voltage of the Fredericksz transition in the smectic C phase exhibits only a weak temperature dependence. In most cases the threshold voltage decreases somewhat with increasing temperature (cf. table 1). For substances with  $S_A$ – $S_C$  polymorphism at first sight a strong decrease of the threshold voltage is expected from equation (12) or (14), because on approaching the second order smectic C–smectic A transition the tilt angle tends to zero. However because  $B$  is proportional to  $\theta^2$  at small tilt angles  $\theta$  [12] the experimentally observed temperature dependence of the threshold field becomes plausible.

#### 4.3. The switching times

In our measurements the rise and decay times are defined as those times for which 50 per cent of the change of the light intensity occurs on applying or removing the electric field. In tables 2–6 the rise and decay times for five materials are listed which were measured in the nematic and smectic C phases at different temperatures and different voltages. The layer thickness in all cases was  $10 \mu\text{m}$ . As we see from the tables, for all the materials studied the decay time in the smectic C phase is clearly shorter than in the nematic phase of the same material. For the compounds C4, C7 and the binary mixture the decay time in the nematic and the smectic C phase differ by about one order of magnitude.



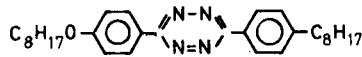
Table 2. The rise and decay times for C6.



Phase	$T/^\circ\text{C}$	$U/\text{V}$	$t_{\text{rise}}/\text{ms}$	$t_{\text{decay}}/\text{ms}$
N	98	25	150	10
		30	90	10
		40	70	9
		50	35	8
S <sub>C</sub>	93	25	14	5
		32	9	5
		40	6	5
		50	4	5
S <sub>C</sub>	77	32	6	3
		40	5	2.5
		50	4	2.5

$$D = 10 \mu\text{m}.$$

Table 3. The rise and decay times for C7.



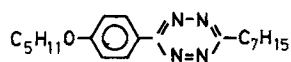
Phase	$T/^\circ\text{C}$	$U/\text{V}$	$t_{\text{rise}}/\text{ms}$	$t_{\text{decay}}/\text{ms}$
N	167	15	15	15
		20	5.5	15
		30	2	15
		40	1.5	15
S <sub>C</sub>	161	25	2.5	1.5
		30	1.5	2
		40	1.0	2
		50	0.7	2
S <sub>C</sub>	132	25	3.5	2
		30	2.3	2
		40	1.3	2
		50	0.8	2

$$D = 10 \mu\text{m}.$$

It is useful to compare the rise time in both phases at the same value of  $(U^2 - U_2^2)$ . Whereas for the compounds C6 and C7  $t_{\text{rise}}$  in the smectic C phase is smaller than in the nematic phase, for the compound C4 and the binary mixture (cf. table 6) the reverse behaviour is found.

The decay and rise times of a continuous Fredericksz transition ( $\mu = 0$ ) can be expressed by equations (16) and (17), respectively. From these equations it follows that neither the decay time nor the rise time depends markedly on the tilt angle  $\theta$ , because  $B$  as well as  $\lambda$  is proportional to  $\theta^2$  at small tilt angles [12]. For the substance C6, where the dielectric reorientation is a continuous transition, the plot of  $t_{\text{rise}}$  against  $(U^2 - U_2^2)$  gives a straight line in accord with equation (17) (see figure 10).

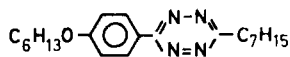
Table 4. The rise and decay times for C3.



Phase	$T/^\circ\text{C}$	$U/V$	$t_{\text{rise}}/\text{ms}$	$t_{\text{decay}}/\text{ms}$
N	54.5	15	80	55
		20	40	60
		30	15	60
		40	7	60
$S_C$	51.5	20	40	10
		30	32	10
		40	21	10
		50	13	10

$$D = 10 \mu\text{m}.$$

Table 5. The rise and decay times for C4.



Phase	$T/^\circ\text{C}$	$U/V$	$t_{\text{rise}}/\text{ms}$	$t_{\text{decay}}/\text{ms}$
N	75	10	60	30
		20	15	35
		30	5.5	35
		40	3	35
$S_C$	65	32	80	1.6
		40	50	1.7
		50	22.5	1.7
$S_C$	56	32	110	1.7
		40	50	1.8
		50	27	1.8

$$D = 10 \mu\text{m}.$$

#### 4.4. Determination of the elastic constant and the rotational viscosity

We have used equations (12) and (14) to estimate the elastic constant  $B$  from the measured threshold voltage provided that the dielectric anisotropy  $\Delta\epsilon$  and the tilt angle  $\theta$  were known. For four substances the estimated values are given in table 7 together with the splay elastic constant  $k_{11}$  of the nematic phase. For the compound C6 the planar orientation of the smectic C phase corresponds to the second borderline case ( $\mu = 0$ ). Therefore the elastic constant calculated from equation (12) is identical with  $B_2$  in the framework of the Rapini theory [1, 9]. For the other substances the first borderline case of planar orientation ( $\mu = \theta$ ) is approximately fulfilled. In this case the elastic constant calculated from equation (14) is an average elastic constant [9].

Although the values of  $B$  and  $k_{11}$  listed in table 7 are quite approximate values the general relations of the order of magnitude of the elastic constants in nematic and smectic C phases are obvious. For all materials studied the splay elastic constant  $k_{11}$  of the nematic phase is higher than the elastic constant  $B$  in the smectic C phase.



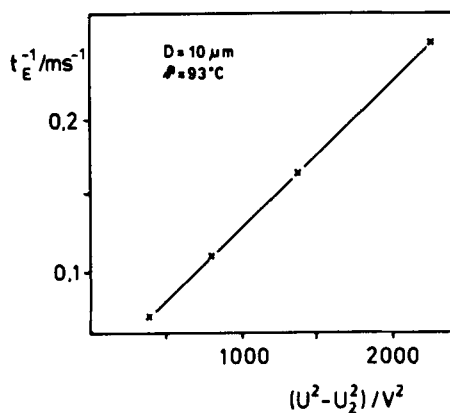
Figure 10. Plot of the reciprocal rise time against  $U^2 - U_2^2$  in the smectic C phase of C6.

Table 6. The rise and decay times for the equimolar mixture.

$$\text{C}_9\text{H}_{19}\text{O}-\text{C}_6\text{H}_4-\text{N}^+\text{N}^--\text{C}_7\text{H}_{15} / \text{C}_{10}\text{H}_{21}\text{O}-\text{C}_6\text{H}_4-\text{N}^+\text{N}^--\text{C}_7\text{H}_{15}$$

K 43.5–44 S<sub>C</sub> 52–52.5 S<sub>A</sub> 56.5–57 N 70–70.3 I [4]

Phase	$T/^\circ\text{C}$	$U/\text{V}$	$t_{\text{rise}}/\text{ms}$	$t_{\text{decay}}/\text{ms}$
N	61	10	110	25
		20	30	25
		30	12.5	25
		40	8	25
S <sub>C</sub>	45	32	30	2
		40	15	2.5
		50	7	2.5
S <sub>C</sub>	31	32	30	3
		40	13	3
		50	8	3

$D = 10 \mu\text{m}.$

Table 7. The elastic constants and tilt angles for four materials.

Compound	Phase	$T/^\circ\text{C}$	$U_2/\text{V}$	$\theta/^\circ$	$\Delta\epsilon$	$k_{11}/10^{-12}\text{N}$	$B/10^{-12}\text{N}$	$B_0/10^{12}\text{N}$
C1	S <sub>C</sub>	31	17.5	28	0.47		11	45
	S <sub>C</sub>	47	17	20	0.47		6.1	50
	S <sub>C</sub>	50	17	12.5	0.46		2.6	55
	N	62	6		0.53	17		
C5	S <sub>C</sub>	69.5	33	12	0.206		4.1	94
	S <sub>C</sub>	71.5	33	7.5	0.207		1.5	88
	N	82	6		0.20	6.5		
C6	S <sub>C</sub>	79	16	15	0.27		4.2	61
	N	100	10		0.45	40		
C9	S <sub>C</sub>	70	15	15	2.4†		15	219
	N	116	4		3.0	43		

† Measured in the smectic A region near the transition to the smectic C phase.

However because  $B$  is directly proportional to  $\theta^2$  [12], it seems to be reasonable to compare  $k_{11}$  with a reduced elastic constant defined as  $B_0 = B/\theta^2$ . It is seen from the table that  $B_0$  is always higher than  $k_{11}$  in the nematic phase. To our knowledge, until now the elastic constant  $B$  was measured for only one substance (4-*n*-hexylphenyl-4-*n*-nonyloxy-benzoate) [21]. According to this measurement  $B$  was found to be  $0.5 \times 10^{-12}$  N at 3°C below the smectic C–smectic A transition, whereas the reduced elastic constant  $B_0$  is about  $10 \times 10^{-12}$  N ( $\theta = 13^\circ$ ). These values are somewhat lower than those determined in our measurements.

From equation (16) we can determine the rotational viscosity  $\lambda$  of the smectic C phase provided that the decay times and the elastic constants are known. This conditions is satisfied for two materials, the compound C6 and the binary mixture of pyrimidine derivatives, listed in table 6. For the binary mixture we have used the elastic constant of the component C1. Table 8 lists the estimated rotational viscosities in the nematic and smectic C phase of the compound C6 and the binary mixture.

Table 8. The rotational viscosity of two materials.

Compound	Phase	$T/^\circ\text{C}$	$\theta/^\circ$	$B/10^{-12}$ N	$t_{\text{decay}}/\text{ms}$	$\lambda/\text{mPa s}$	$\lambda_0/\text{mPa s}$
C6	$S_C$	93	15	3.2	5	1.6	23
	N	100		40	10	39	
Binary mixture	$S_C$	31	28	11	3	3.2	13
	$S_C$	45	22	7.3	2.5	1.8	12
	N	61		17	25	42	

It is seen from table 8 that the rotational viscosity of the nematic phase is considerably higher than that of the smectic C phase. It must be considered that the viscosity is also proportional to  $\theta^2$  for small tilt angles [12]. However the reduced rotational viscosity,  $\lambda_0 = \lambda/\theta^2$ , is also lower than in the nematic phase.

Until now the rotational viscosity of smectic phases was measured for only a few substances, and the results of the measurements are contradictory. Meiboom and Hewitt [22], also Skarp *et al.* [23] found values which are about one order of magnitude higher than our values and than those of Kuczynski [21] and Rosenblatt *et al.* [24]. The reasons for this discrepancy are not known. None the less it should be noted that in agreement with our results Meiboom and Hewitt [22] measured a higher value of the rotational viscosity in the nematic phase than in the smectic C phase.

### References

- [1] RAPINI, A., 1972, *J. Phys., Paris*, **33**, 237.
- [2] MEIROVICH, E., LUZ, Z., and ALEXANDER, S., 1977, *Phys. Rev. A*, **15**, 408.
- [3] PELZL, G., SCHUBERT, H., ZASCHKE, H., and DEMUS, D., 1979, *Kristall Technik.*, **14**, 817.
- [4] PELZL, G., KOLBE, P., PREUKSCHAS, U., DIELE, S., and DEMUS, D., 1979, *Molec. Crystals liq. Crystals*, **53**, 167.
- [5] FREDERICKSZ, V., and ZOLINA, V., 1931, *Z. Kristallogr.*, **79**, 225.
- [6] DE GENNES, P. G., 1974, *The Physics of Liquid Crystals* (Oxford University Press).
- [7] SCHILLER, P., PELZL, G., and DEMUS, D., 1987, *Liq. Crystals*, **2**, 21.
- [8] SAUNDERS, P. T., 1980, *An Introduction to Catastrophe Theory* (Cambridge University Press).
- [9] SCHILLER, P., and PELZL, G., 1983, *Crystal Res. Technol.*, **18**, 923.
- [10] PELZL, G., HAUSER, A., KRESSE, H., and DEMUS, D., 1980, *Kristall. Technik.*, **15**, 1345.
- [11] HAUSER, A., KRESSE, H., PELZL, G., and DEMUS, D., 1981, *Crystal Res. Technol.*, **16**, 1055.
- [12] DIEGO, A. C., and MARTINS, A. F., 1980, *Liquid Crystals of One- and Two-Dimensional Order*, edited by W. Helfrich and G. Heppke (Springer-Verlag), p. 108.

- [13] ZASCHKE, H., 1975, *J. prakt. Chem.*, **317**, 617.
- [14] ZASCHKE, H., and STOLLE, R., 1975, *Z. Chem.*, **15**, 441.
- [15] DEMUS, D., KRÜCKE, B., KUSCHEL, F., NOTHNIK, H.-U., PELZL, G., and ZASCHKE, H., 1979, *Molec. Crystals liq. Crystals Lett.*, **56**, 115.
- [16] PELZL, G., SHARMA, N. K., RICHTER, L., WIEGELEBEN, A., SCHRÖDER, G., DIELE, S., and DEMUS, D., 1981, *Z. phys. Chem.*, **262**, 815.
- [17] PELZL, G., 1980, *Kristall. Technik.*, **15**, 349.
- [18] ZASCHKE, H., DEBAQ, J., and SCHUBERT, H., 1975, *Z. Chem.*, **15**, 100.
- [19] WEIßFLOG, W., PELZL, G., WIEGELEBEN, A., and DEMUS, D., 1980, *Molec. Crystals liq. Crystals Lett.*, **56**, 295.
- [20] WEIßFLOG, W., MÖCKEL, P., KOLBE, A., KRESSE, H., PELZL, G., MOHR, K., and ZASCHKE, H., 1984, *J. prakt. Chem.*, **326**, 457.
- [21] KUCZYNSKI, W., 1981, *Ber. Bunsenges. phys. Chem.*, **85**, 234.
- [22] MEIBOOM, S., and HEWITT, R. C., 1975, *Phys. Rev. Lett.*, **34**, 1146.
- [23] SKARP, K., DAHL, I., LAGERWALL, S. T., and STEBLER, B., 1984, *Molec. Crystals liq. Crystals*, **114**, 283.
- [24] ROSENBLATT, C. S., PINDAK, R., MEYER, R. B., and CLARK, N. A., 1980, *Phys. Rev. A*, **21**, 140.